6
SOLID EARTH MODELLING PROGRAMME

Solid Earth Modelling Programme's (SEMP) research focus is integration of GNSS, Computational seismology, tectonics, geology, ground motion modeling for quantification of natural hazard (earthquake, landslides, extreme events) specific to Indian subcontinent (Indian Himalayas, Northeast India and Rigid Indian Plate). This programme is multidisciplinary (Engineering and Earth Sciences) and multi-component. Some of the major contributions during the year 2015-2016 are establishment of Multi-parameter (GNSS and Broadband seismic) observation network in Kashmir Himalaya, GPS based landslide deformation modelling, preliminary estimate of Indian reference frame, spatio-temporal variability of GPS-PWV and GPS-TEC specific to Indian subcontinent. Broadband seismic network in Kashmir Himalaya gave first crustal shear velocity model of the intermontane Kashmir valley longitudinally carved within the northwestern Great Himalaya barely 70 km to the southeast of the Hazara syntaxis. In addition Unified Scaling Law for Earthquake (UCLE) has been applied to model the earthquake hazard and convolved with population density to image the risk model of Gujarat. Probabilistic earthquake hazard assessment in Peninsular India has been completed. During this period, two PhD's were awarded and the group has about 150 citations for their research publications. We network with large number of premier institutions in the country and abroad and scientists of this group serve as expert members in several national and international committees.

Inside

- *GPS-TEC Estimation*
- *Establishment of Continuous mode Global Navigation Satellite System (CGNSS) network in Kashmir Valley*
- *Landslide studies using Global Positioning System (GPS)*
- *Modelling of Landslides using Finite Element Method (FEM)*
- *Digital Elevation Model(DEM) for Landslide Studies*
- *GPS measurements in landslides, Uttarakhand*
- *Seismic hazard and risk assessment based on the Unified Scaling Law for Earthquakes: State of Gujarat, India*
- *Crustal Structure and seismicity beneath Kashmir Himalaya*
- *Moho Imaging in Dharwar craton*
- *Strong ground motion estimation in Western Himalaya & adjacent areas*
- *Study of Tank with Inclined Braced Staging*
- *Adaptive Nonlinear Pushover Analysis on L-Shaped Building*

6.1 Estimation of Indian reference frame from CGPS network analysis

Indian GPS network data from GPS sites established by us and our collaborators are analysed for a period of 17 years (1997-2014) using GAMIT/GLOBK along with IGS stations as shown in figure 1. Daily loose GAMIT solutions with their covariance matrix were obtained which are then combined using GLORG for reference frame definition by stabilizing the IGS sites to their ITRF08 coordinates and velocities. To account for errors in modeling the orbits and atmosphere in the long time series and time correlated sources of errors in position estimates including monument instability, we included random-walk noise at the level of 2 mm/year in the coordinates for all stations during the GLORG reference frame stabilization. The positions and velocities of all the GPS sites were thus obtained in the ITRF08 reference frame. GPS times series in North, East, Upthus obtained for one sample site located in Hanle, Ladakh is given in figure 6.2. ITRF2008 velocities thus estimated from rigorous global analysis along with error ellipses are given for all the sites in figure 6.1.

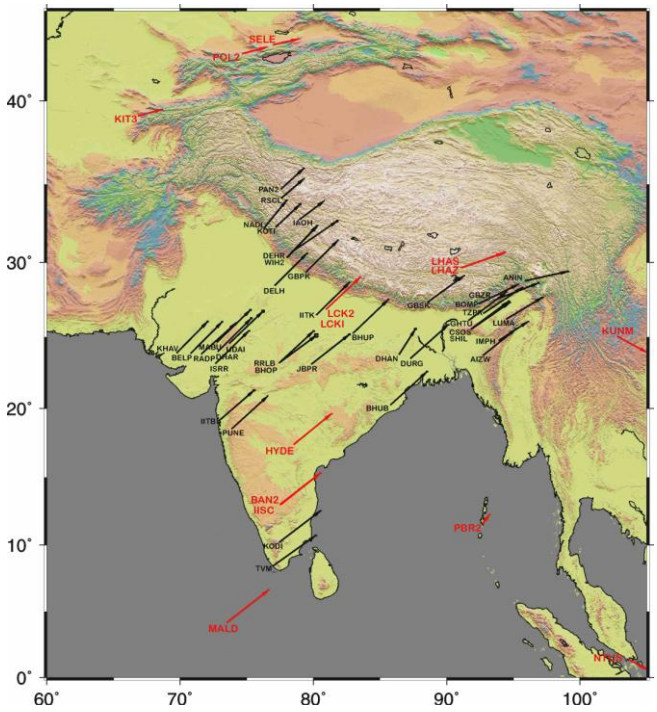

Figure 6.1 ITRF2008 velocities estimated from GPS global data analysis for 17 year period

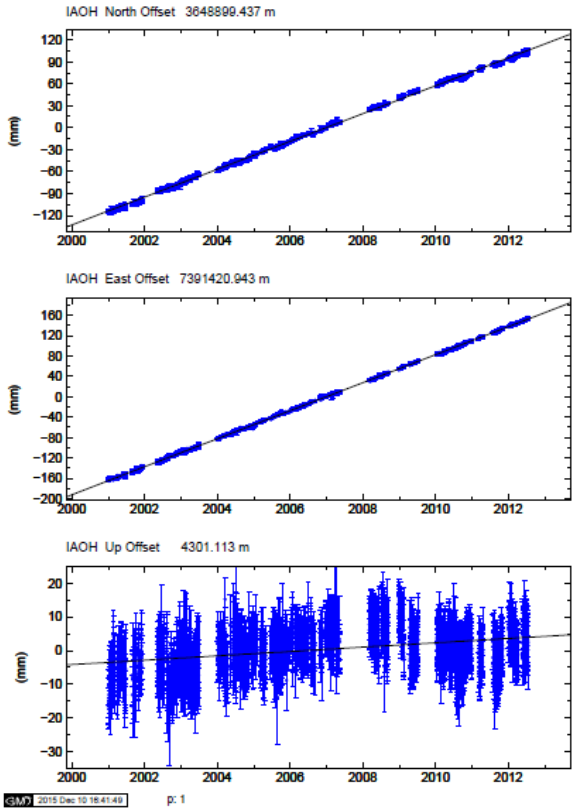

Figure 6.2 North, East and Up times series of Hanle station from 2000-2012

Using the ITRF08 GPS site positions and velocities of sites located onrigid Indian plate and Maldives IGS site located in Indian Plate, Indian reference frame is estimated using GLORG and the euler pole of rotation of Indian Plate in ITRF2008 thus estimated is located at 52.449±0.225°N, 1.145±1.200°E with angular velocity of 0.499375±0.004731.

Sridevi Jade and Shrungeshwar T S

6.2 Inverse modelling of GPS horizontal surface velocities in Northeast India

GPS derived velocity field in Shillong Plateau, Assam Valley, Eastern Himalaya and Indo-Burmese Arc using GPS measurements spanning 11 years (2002-2013) is used for modelling the region-specific deformation field. Inverse modelling is based on the Okada dislocation theory and weighted least-square inversion. The best fit model is the one for which the residual between the observed and modelled displacements is minimal. Computations are performed iteratively yielding the final dislocation parameters that best match the GPS observed surface deformation pattern. The inverse model thus obtained gives constraints on the geometry and the slip of the sub-surface dislocations which cause the surface horizontal deformation. These models give significant insights into the strain accumulation and stress buildup in this tectonically active region.

Sridevi Jade, Shrungeshwar T S, Prakash Barman

6.3 Computation of strain rates from GPS displacements

GPS derived ground displacements at tectonic plate, regional and local scale are used to study the tectonic effects (crustal deformation) as well as kinematics of a single landslide. Crustal deformation is determined from analysis of GPS ground observations from a continuous and campaign network of GPS stations spatially distributed over the study region. Precise time series of positions/displacements in north, east and up obtained from the analysis of GPS data is used to determine the crustal strain rates at tectonic scale, regional strain rates across faults and slow relative motion of landslide at a local scale. A set of multi-temporal coordinates of experimental points (EPs) are used to get the information on the kinematics. Strain rates at different scale i.e., from tectonic plate, regional and local scale can be estimated from a given GPS displacements (or velocity) data set. The GPS strain analysis is carried out using Lagrangian approach, wherein it starts with an initial configuration and projects to a final deformed configuration. Two dimensional deformation rate field is calculated in a region, starting from the velocities of a series of observational points (EPs) adequately distributed in this region. The input data are the velocities derived by the processing of field GPS measurements. At each location, a uniform strain rate field is assumed, and a least squares inversion is performed over strain velocity solutions and their covariance for six unknowns to estimate the strain. The obtained deformation pattern is a set of the principal components of the strain calculated on a regular grid. A trial run to compute the strain rate from the published GPS displacements and velocities has been performed.

Pavithra N R and Sridevi Jade

6.4 Spatial and temporal variability of GPS derived PWV

The radio signals transmitted from GPS satellites to the ground receivers are delayed in the atmosphere and such delay in the troposphere i.e., Zenith Total Delay (ZTD) gives a crucial parameter to estimate the Precipitable Water Vapour (PWV) from GPS data. Zenith Total Delay (ZTD) consists of Zenith Hydrostatic Delay (ZHD) and Zenith Wet Delay (ZWD).To derive PWV from ZTD, required surface pressure and temperature values were taken from Meteorological sensors collocated adjacent to GPS receivers. The Meteorological sensors record temperature and pressure at a 5 sec interval with 0.2ppm accuracy. The errors associated with GPS PWV estimates depend on the (i) uncertainty associated with estimation of Zenith Total Delay (ZTD) from GPS observations, (ii) accuracy of the observed surface pressure and temperature values recorded by meteorological sensors and (iii) weighted mean temperature of the atmosphere. Several studies were conducted to estimate the absolute and relative errors in PWV associated with errors in ZTD, P and T_m by taking partial derivatives of the above equations and concluded that the accuracy of PWV estimated by GPS is about 2-3 mm at various locations of the Indian subcontinent. For dry sites with low PWV values, the ZTD is almost completely due to ZHD and small errors in ZTD and ZHD would contribute to large errors in ZWD i.e., (ZTD-ZHD) and in the retrieval of GPS PWV. GPS PWV thus estimated for the Indian network for all the GPS sites collocated with met sensors during 2001-2013 is given in figure 6.3.

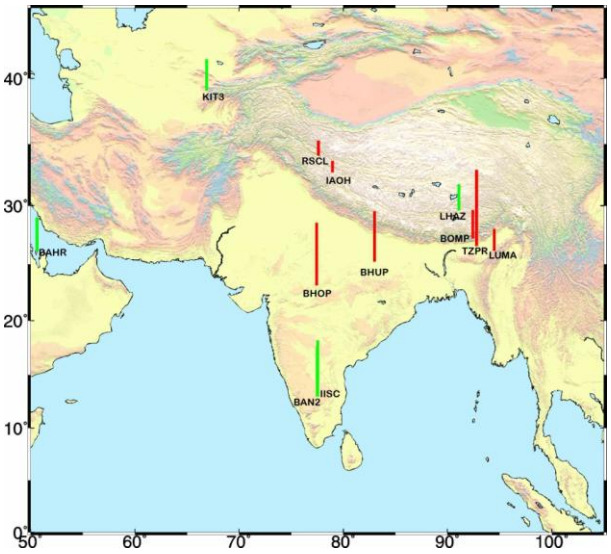

Figure 6.3 Mean GPS-PWV column estimated for a 13 yr period at GPS sites with collocated Met-Sensors

Mean GPS PWV (figure 6.5) of Indian GPS sites varies between 6mm at high altitude (4500m) Hanle site to 44 mm at Tezpur site in northeast India located almost at the (120m) MSL height.

Interannual, seasonal, diurnal variability of PWV has been studied for all the sites and results for high altitude Hanle site for a period of 8 years are dicussed here. The Yearly mean PWV of Hanle site is ~ 4.2 mm for all the years except for slightly higher PWV of ~4.9 mm for 2006 and lower PWV for

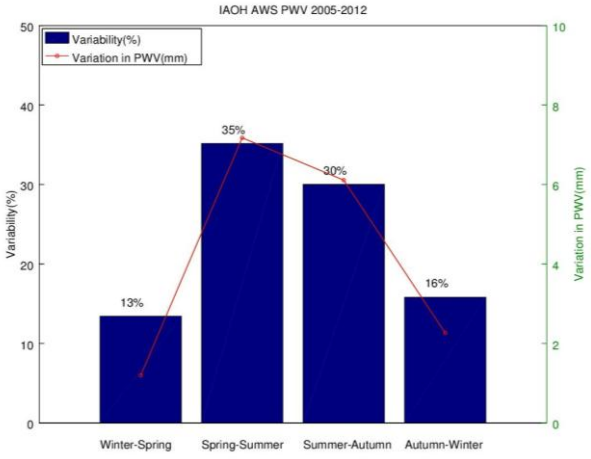

Figure 6.4 Inter-seasonal variability of GPS-PWV for 8 year period

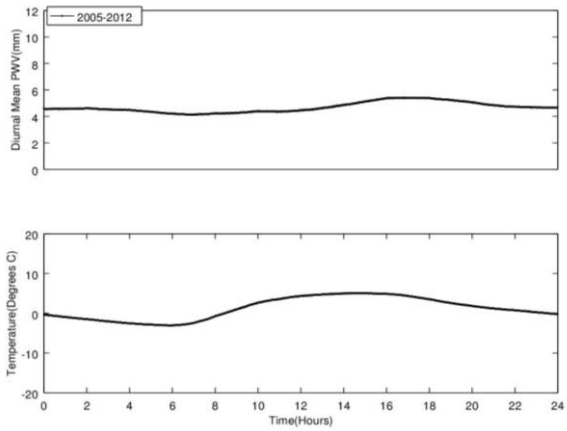

Figure 6.5 Diurnal Variability of GPS-PWV estimated at 30 sec interval for a eight year period along with surface temperature recorded at 5 sec interval.

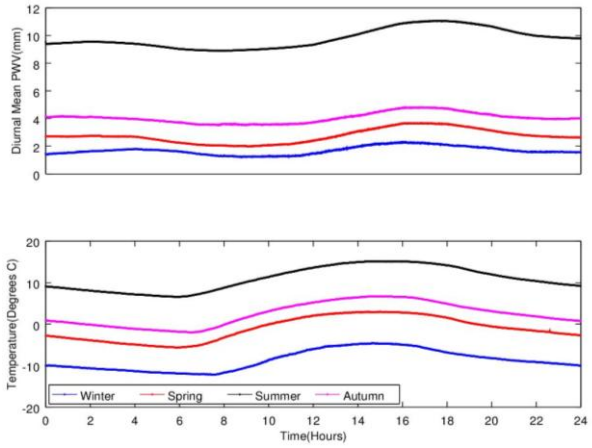

Figure 6.6 Seasonal diurnal variability of GPS PWV and surface temperature

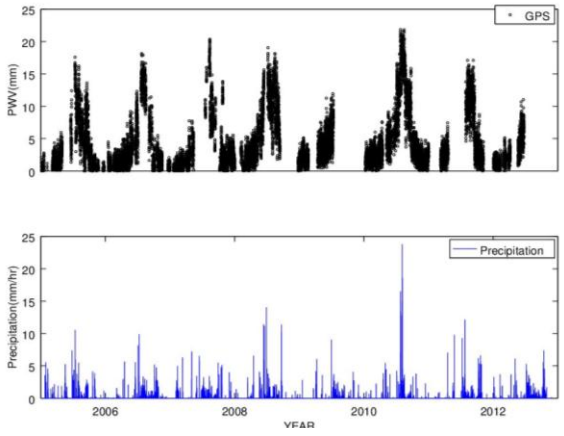

Figure 6.7 GPS-PWV at 30 sec interval for eight year period along with TRMM precipitation.

~3.6mm for 2009. High average PWV for 2006 coincides with the record highest rainfall of 131 mm received at Hanle during the year. Low PWV in 2009 is due to the low rainfall of ~80 mm during this year. Rest of the years received average rainfall of 105 mm and hence the PWV is consistent with this value. The season to season variability of GPS PWV (2005-2012) is plotted in figure 6.4. The results indicate percentage variability between winter-spring-autumn is almost half of the value of Spring-Summer-autumn which is typical of high altitude sites with dry weather.

GPS-PWV is estimated every 30 sec for the eight year period (2005-2012) and has been plotted in the figure 6.5to study the diurnal variability of PWV at Hanle. PWV at this site indicates a very distinct diurnal variability which peaks at 16-18 hr of the day with a low value at 6-8 hr which is consistent with the day time temperatures in this region. Season wise diurnal variability is also plotted along with the temperature in figure 6.6.

Precipitation (mm/hr) is estimated from The Tropical Rainfall Measuring Mission (TRMM, 3B41RT version 7data products from http://gdata1.sci.gsfc.nasa.gov/) with spatial resolution of 0.25 X 0.25° grid averaged over Hanle site. This data is compared with 30s interval GPS PWV estimated at Hanle and is shown in figure 6.7 which indicates a similar trend between the two parameters during the eight year period. The peak values of precipitation coincide with the peak values of 30s PWV estimated from GPS. The high precipitation for all the years occurs during July–August which is due to high moisture content n the atmosphere as a result of high temperature and relative humidity at site during these months.

6.5 Validation of water vapor retrieval from MODIS using GPS PWV over IAO-Hanle, in trans-Himalayan Region

Integrated PWV retrieved from Moderate Resolution Imaging Spectro-radiometer (MODIS) in near-infrared channels is examined with the PWV estimated from the Global Positioning System (GPS) data with measured surface temperature and pressure values over Hanle, located at a high-altitude (~4500m) trans-Himalayan region. Since the accuracy of MODIS derived PWV over the large elevated topography of the region is not well studied, the present work focus is on the validation of MODIS PWV using the GPS data during 2005-2012.

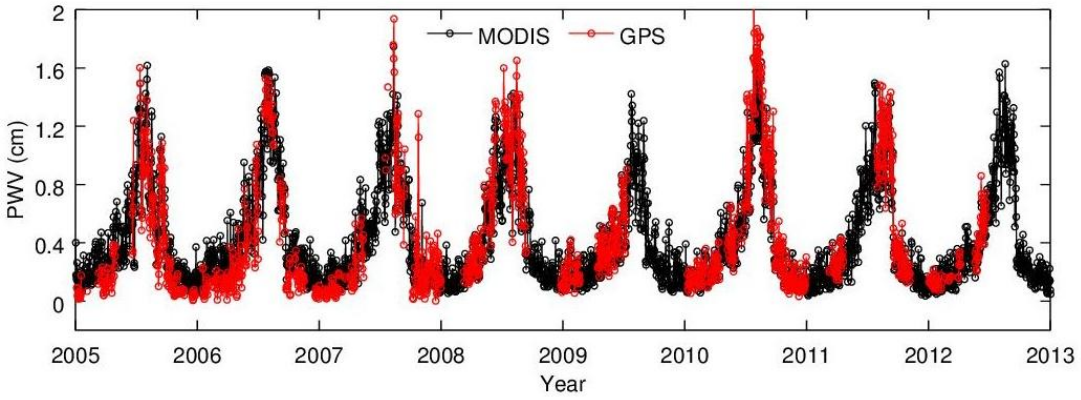

Figure 6.8 Daily PWV(cm) between the MODIS and GPS data

The study reveals that MODIS PWV compares well with the GPS PWV data with bias -0.018 cm, root mean square error (RMSE) 0.137 cm and coefficient of determination (R^2) 0.91. The two types of data products are compared (Figure 6.8) on short (daily) and long temporal (monthly-seasonal) scales in order to evaluate the seasonal dependence of PWV. The peak values of PWV from MODIS and GPS data at the site varied from 1.7 to 2.05 cm and 1.2 to 1.4 cm as the daily and the monthly means, respectively which occurred during August. However, the seasonal peak of PWV occurred during summer as 0.88 and 0.97cm for MODIS and GPS data, respectively. The present study noticed that about 85% of the total PWV estimated from MODIS as well as GPS data lies below 1.0 cm over the site. The seasonal study of PWV reveals that MODIS data is found to be underestimating the PWV when compared to GPS data with bias -0.095 cm and RMSE 0.215 cm particularly during summer. This is due to dry and high-altitude terrain of Hanle particularly during summer months. However, there are marginal differences (bias varied from 0.007 to 0.017 cm) during the remaining seasons and seasonally R^2 varies from 0.62 to 0.87. Total rainfall over Hanle is recorded from the AWS installed at the site and the measured rainfall during year 2006 and 2010 follows similar trend with good correlation when compared with MODIS and GPS PWV estimated at the site. PWV estimated at Hanle for the year 2010 indicate a peak PWV of ~1.4 cm during August with daily peak value of 2.05 cm which coincides during Leh cloud-burst in August 2010.

Ningombam S, Sridevi Jade and Shrungeshwara T S

6.6 MODIS, ERA-Interim and GPS PWV

PWV is the total water vapor contained in an air column from the Earth's surface to the top of the atmosphere. Atmospheric water vapor is highly variable in both space and time across Earth, and knowledge of distribution of water vapor is essential in understanding weather and climate studies. The Moderate Resolution Imaging Spectro-radiometer (MODIS) is the first space instrument to obtain PWV with near-infrared (NIR) bands and the traditional IR bands, which provides an opportunity to monitor PWV with wide coverage during both daytime and night time. However, the accuracy of PWV Measurements obtained with IR bands is much lower than that with NIR bands. Global Positioning System (GPS) is another practical tool for measuring PWV on a global basis, which uses the delay in radio signals due to the permanent dipole moment of atmospheric water vapor molecules to infer PWV The advantages of the GPS-derived PWV are continuous measurements in all weather conditions, high accuracy long-term stability and low cost. In addition to GPS and MODIS, ECMWF (European Centre for Medium Range Weather Forecast) data with good spatial resolution ($0.75^0 \times 0.75^0$) is used to retrieve PWV. In this study PWV is retrieved using MODIS NIR with $1^0 \times 1^0$ resolution in day time and ERA-Interim (ECMWRF) with $0.75^0 \times 0.75^0$ horizontal resolution. Gridded data from ECMWF and MODIS are interpolated to the specific latitude and longitude of GPS station to obtain precise PWV values. PWV thus obtained is compared with GPS-PWV estimated for every 2 hours using continuous GPS data in India for a period of 11 years (2002-2013). Sample comparison plot for Bangalore IGS station is given in the Figure 6.9.

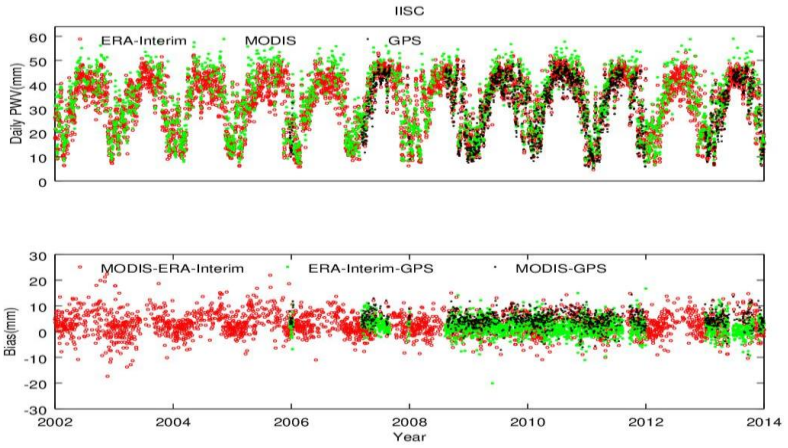

Figure 6.9 Comparison of MODIS, ERA-Interim and GPS PWV (Perceptible Water Vapor) at IISC, IGS site located at Bangalore for a 12 year period.

Sridevi Jade, Boddapati Anil and Shrungeshwara T S

6.7 Assimilation of GPS PWV and ZTD in WRF-NWP model

Accurate and reliable weather forecasting is important for agriculture, aviation and many other human activities. Accuracy of weather forecast can be improved by assimilation of atmospheric PWV into Numerical Weather Prediction (NWP) model. In Convective and Orographically-induced Precipitation Study (COPS) over Europe, assimilation of GPS ZTD has shown clear positive impact on the precipitation forecasting. In Turkey, assimilation of GPS PWV for three specific heavy snow case indicated reduction in the biases and improvement in precipitation

forecasts. Impact of GPS-PWV and ZTD assimilation in Weather Research and Forecasting (WRF)-NWP model by Central Weather Bureau, Taiwan during typhoon Kalmaegi gave 29% reduction of the forecast error during first 6-hr rainfall forecast. In India, an attempt is made for the first time to assimilate PWV and ZTD estimated using nationwide GPS data into the WRF model. The WRF Model is a next-generation mesoscale NWP model designed for both atmospheric research and operational forecasting needs. WRF can generate atmospheric simulations using real data (observations, analyses) or idealized conditions. WRF offers operational forecasting a flexible and computationally-efficient platform, while providing recent advances in physics, numerics, and data assimilation. WRF is currently in operational use at NCEP, AFWA, and other centers. The accuracy of the WRF output will be assessed by comparing the model forecast data with in-situ observations. Any improvement in forecasting capability is highly desirable for Indian Agrarian economy. The experiment is expected to yield strengths and short-comings of the assimilation on forecast and also help to tune the WRF model for Indian region.

Sridevi Jade and Prakash Barman

6.8 GPS-TEC estimation

Four GPS observables, carrier phase delays L1 and L2 and code pseudorange group delays P1 and P2 expressed in range units are used for GPS TEC (Total Electron Content) estimation. GPS data analysis using GAMIT is used to extract the ionosphere delay of GPS observables from the one-way residuals for each PRN i.e. satellite after cleaning the data. These are used to derive the Slant Total Electron Content (STEC) and VTEC which is termed as TEC is given by

$TEC=VTEC= STEC\ (H_{ion}/L_{\theta})$

Where H_{ion} is the mean ionosphere thickness and L_{θ} is ray path length

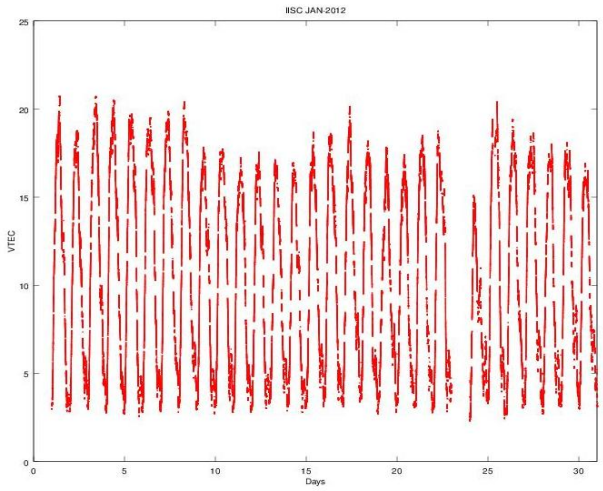

Figure 6.10 Daily variation of GPS TEC at IISC, Bangalore

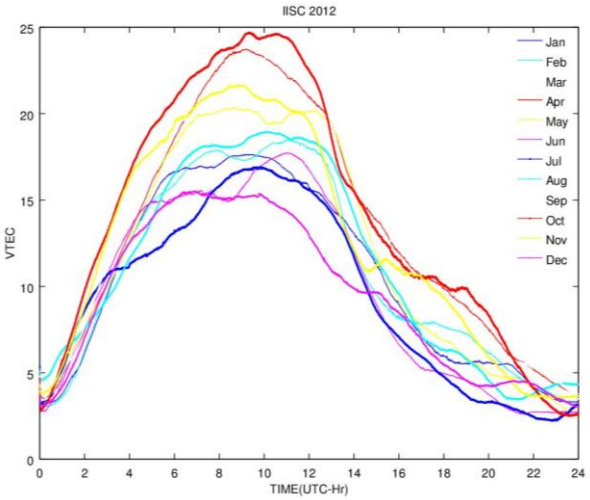

Figure 6.11 Seasonal and diurnal variation of GPS TEC at Bangalore

TEC thus estimated for Indian GPS sites is used to study the spatial, inter-annual, seasonal and diurnal variability of ionosphere over Indian subcontinent. Daily variability of TEC for a period of 30 days in January for IGS station in Bangalore is given in Figure 6.10. Diurnal and seasonal variability of GPS-TEC for a one year period is given in Figure 6.11 which indicates that the time of occurrence of diurnal peak of TEC varies with the season, This study gives significant insights into the variability of TEC which exhibits features like annual, semiannual and day-to-day variability, equatorial noon time variation and equatorial ionization anomaly. In-depth study of variability of GPS-TEC over Indian subcontinent is required to identify ionospheric anomalies and their association with seismic activity.

Sridevi Jade and Shrungeshwar T S

6.9 Establishment of continuous mode Global Navigation Satellite System (CGNSS) network in Kashmir Valley

Kashmir Valley lies in one of the most seismically active regions of India. The knowledge presently available on strain build-up, release and occurrence of earthquake is not adequate enough to assess the seismic vulnerability of the Kashmir valley. Strain build-up when combined with the seismic activity and geodynamics of the region gives information on seismic gaps. To estimate strain and surface deformation in Kashmir Himalayas, establishment of Continuous mode Global Navigation Satellite System (CGNSS) stations in Kashmir Valley is envisaged in collaboration with University of Kashmir, Srinagar, Jammu & Kashmir. CGNSS stations are equipped with geodetic grade dual frequency receivers that observe signals from most of the available GNSS satellites constellations (GPS, GLONASS, Galileo, BeiDou, QZSS). Receiver setup is housed inside the room and antenna is mounted over the RCC pillar as shown in figure.

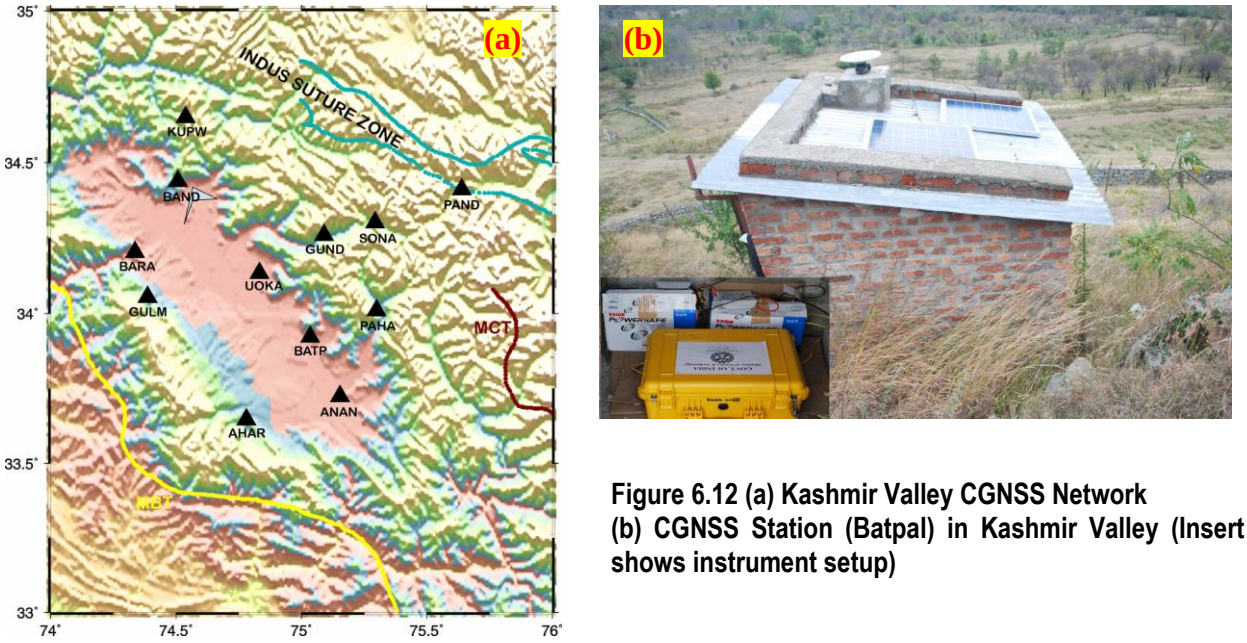

Figure 6.12 (a) Kashmir Valley CGNSS Network (b) CGNSS Station (Batpal) in Kashmir Valley (Insert shows instrument setup)

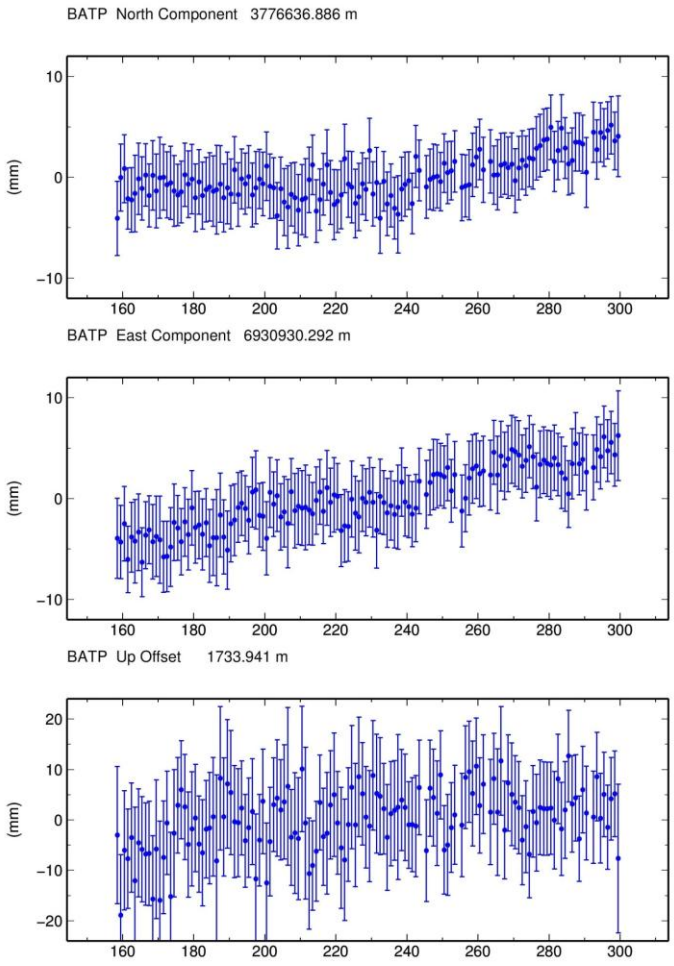

Figure 6.13 Batpal Time Series

Also GNSS data of higher sampling rate of 1 Hz is collected for these stations. Pre-Seismic, Co-Seismic and Post-Seismic motion can be captured using high sampling rate GNSS data. From May to November 2015, twelve CGNSS stations are established along the arc-normal transects in Kashmir valley as shown figure6.12. Two stations are collocated with meteorological sensors. The data collected at these sites is analysed and the daily precise position in North, East and Up with error bars is estimated. Sample time series plot for Batpal station is given in Figure6.13. These daily positions over a period of one year would give the precise velocity estimate of these sites in ITRF08 reference frame and the relative motion between the sites gives the surface deformation rates in Kashmir Valley.

Chiranjeevi Vivek G, Suri Babu D,
Ramees Raja Mir, Dharma Teja A K,
Sunil Babu M G, Niranjan N, Parvez I A,
Sridevi Jade & UOK team

6.10 Landslide studies using Global Positioning System (GPS)

Gharwal Himalayas falls in seismic zone-V and also in high hazard zone. In the upper reaches of Alaknanda valley of Gharwal Himalayas, there are several landslide potential zones along the Chamoli-Badrinath National Highway (NH-58), Uttarakhand. NH-58 is a landslide prone zone due to the adverse geological formation, steep slopes, highly dissected topography, seismically active area and high rainfall. CSIR-Central Building Research Institute (CBRI) in collaboration with CSIR-4PI has selected two landslides in Jalgwar village, Chamoli district, Uttarakhand for monitoring. These landslides are of debris slide types with minor rock slides at the flanks (Figure 6.14). Area is also in the vicinity of Main Central Thrust (MCT) which is seismically active. Main cause of the slide is due to very highly weathered dolomites on a steep slope and the rock formation is highly crushed at several places.

Figure 6.14 View of Landslides

Figure 6.15 Continuous, reference and control GPS stations (clockwise from left)

For the first time in India, specific landslides (Figure 6.15) are studied using Global Positioning System (GPS). GPS measurements were conducted to measure the overall landslide motion and inter-landslide motion. Continuous mode GPS (CGPS) station (CBRI) was established in CBRI campus, Roorkee which runs throughout the year and Campaign mode reference station (LSLI) was established in relatively stable region within aerial distance of 1 Km from landslides which runs only during GPS measurements period in landslides (Figure 6.16). These CGPS station and campaign mode reference station were used to define a stable reference frame to measure the displacement solely due to the landslide motion. Landslide control points (Figure 6.17) are established in landslide 1 and landslide 2 to measure the overall landslide motion as well as deformation within the landslide (Intra Landslide motion).

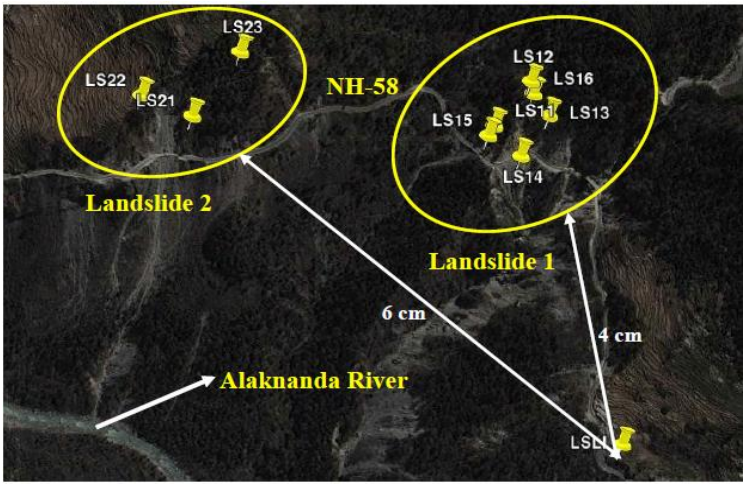

Figure 6.16 Landslides with GPS control points and reference station (LSLI)

GPS data is analysed to determine the precise positions of CBRI, LSLI and landslide control points along with the velocities and rate of change of baseline lengths between the GPS points. Results indicate shortening between CBRI continuous station at Roorkee and reference station (LSLI) inferring long term tectonic motion since CBRI station is at foot hills of Himalayas and LSLI station in transition zone of lesser and higher Himalayas. Baseline length changes between landslide control points and reference station gives the overall motion of the order of 4 cm and 6 cm for landslide 1 and landslide 2 respectively (Figure 6.16). Deformation rates within the landslide vary from 2 to 5 cm in the different sections of the landslides.

Shrungeshwara T S, Chiranjeevi Vivek G,
Anil Kumar Maletha, Shantanu Sarkar and Sridevi Jade

6.11 Modelling of landslides using Finite Element Method (FEM)

Use of finite element method using solvers like ansys, abaqus, hyper mesh to model the landslides under both static and dynamic failure conditions have greatly increased recently. In order to gain the realistic results which can be a base for predicting Landslide movement, the model specifications should be selected in a way close to natural conditions. However in any numerical modelling, there exists some divergences between model and prototype which are inevitable, the loading condition, surrounding soil and boundary condition are selected as close as an actual movement of a slope. Towards this two field cross sections CD and MN of landslide 1 are modeled using finite element program ABAQUS. Two sections are created using the geometry and the soil properties given by field observations and material properties are assigned for the multiple layers consisting of sandy silt, sandy gravel, weathered dolomite,

Parameters used are Young's modulus, cohesion and angle of friction between layers of landslides, density, Poisson's ratio, soil porosity. The interactions between different layers are kept as friction surfaces acting as rough surface.

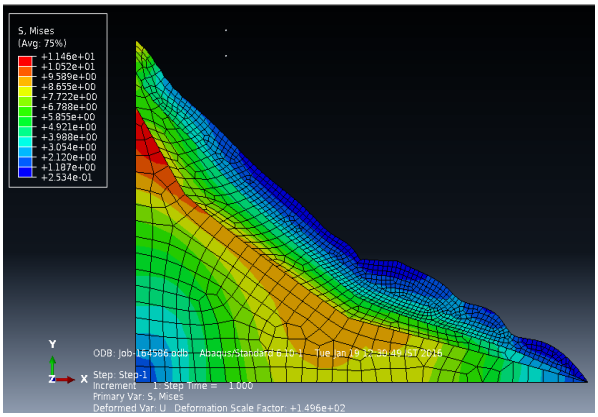

Figure 6.17 (a) Von misses stress distribution for CD Profile

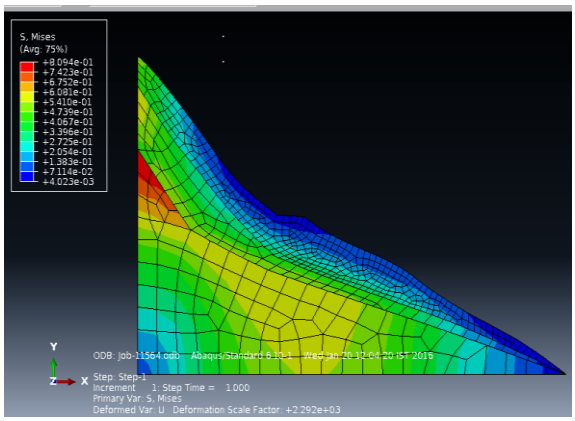

Figure 6.17 (b) Von misses stress distribution for MN Profile

Finite element analysis is carried out with two base steps. At the first step the gravity forces from material density of different layers is calculated and the model is in equilibrium state and stable in static condition, as the study is focused on the dynamic instability of the slope. The second step of the analysis will be started by imposing the dynamic excitation. Forces and loads acting on the slides are given accordingly keeping gravity as main concentrated force acting along whole part. Landslide-1 FEM model was generated for the MN and CD profiles. Displacement magnitude and strain rates obtained using FEM are consistent with GPS in-situ measurements. *Corresponding stress* distribution using the FEM in the multiple layers of landslide for the two cross sections is given in figure 6.17 a and b.

Sridevi Jade, Dharma Teja A K and Kokilagadda Swathi

6.12 Digital Elevation Model (DEM) for landslide studies

DEM is a Digital model or 3D representation of a terrain surface created from terrain elevation data and it could be acquired through various techniques such as Photogrammetry, Lidar, Land surveying, Remote sensing techniques etc.. DEM models are used often in Geographic Information Systems (GIS) and Global Positioning System(GPS). They are the most common basis for digitally produced slope map, aspect map, hill shade map, relief map and contour map. SRTM (Shuttle Radar Topographic Mission-Figure 6.18) DEM of 3 arc-second (90 meter) resolution is used to generate Slope and Aspect map of landslide study area consisting of two landslides in Jalgwar village, Chamoli district, Uttarakhand, using Arc GIS software as shown in Figure 6.18. It gives the information about elevation of study area and it shows landslide points are placed in range of 1497 m to 1567 m elevation with respect to MSL (Mean Sea Level).

Figure 6.18 Slope and Aspect Map of the landslide study region

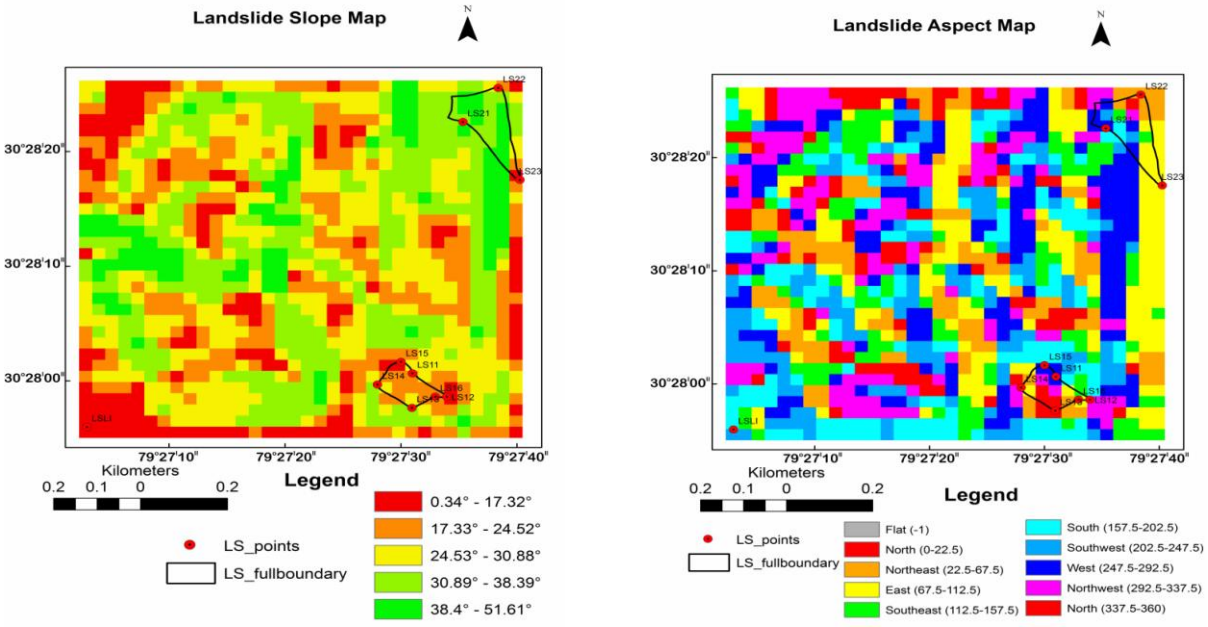

Slope map indicates the topography of an area and gives the measure of steepness or the degree of inclination of a feature relative to the horizontal plane and it can be expressed either in degrees or as a percentage. Aspect map gives the direction of the slope for a terrain and measured clockwise in degrees from 0 to 360, where 0 is north-facing, 90 is east-facing, 180 is south-facing, and 270 is west-facing. Using DEM it is possible to detect minor change in terrain height. Topographic parameters (coordinates and area) derived from DEM is being used in further refinement of Finite Element Model of the landslide.

Sridevi Jade, Sunil Babu M G and Shrungeshwar T S

6.13 GPS measurements in landslides, Uttarakhand

Two epochs of GPS re-measurements were carried out in March, 2015 and October, 2015 in the landslide region located in Jalgwar village, Chamoli district, Uttarakhand. As a part of this continuous mode Global Navigation Satellite System (CGNSS) receiver (CBR1) installed in March 2015 at CSIR-CBRI Campus was upgraded and presently tracks most of the available GNSS constellations. Earlier station (CBRI) was dismantled. This station is made accessible over the internet for remote access, management and data download. CGNSS station is collocated with Meteorological sensor which gives temperature, relative humidity and atmospheric pressure. GPS observations at both the continuous sites are analyzed in static

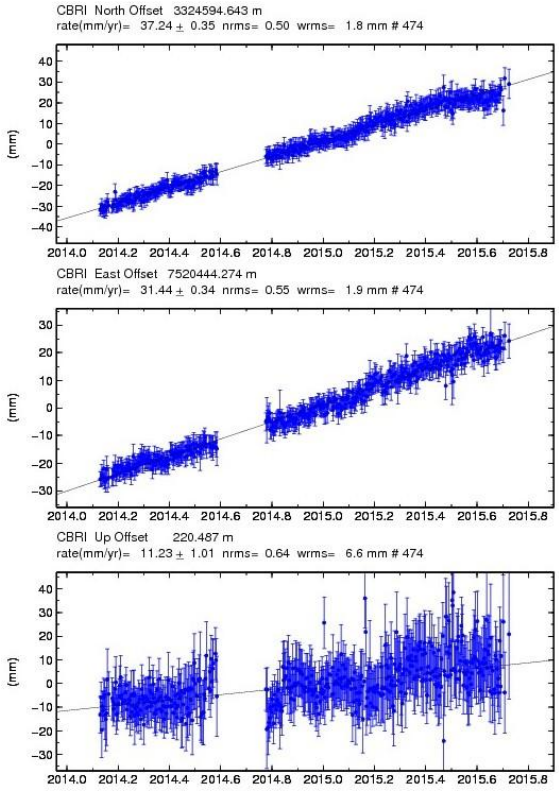

Figure 6.19 (a) CBRI (CGPS) Time series

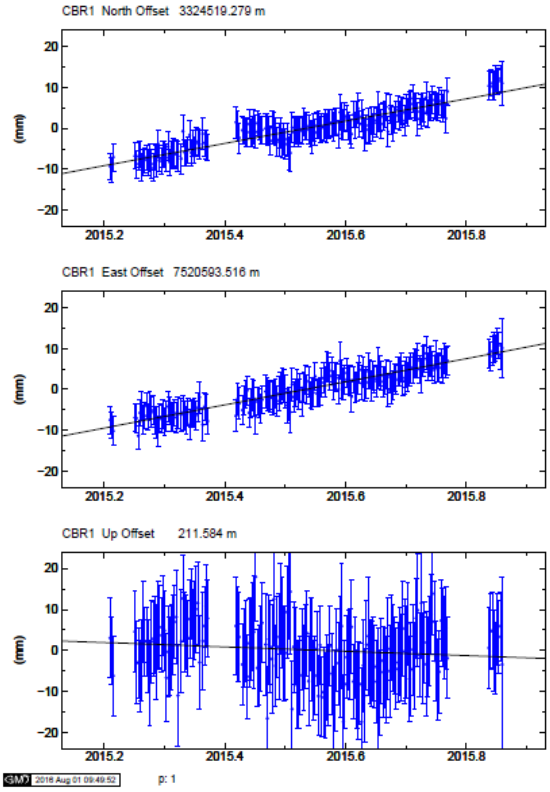

Figure 6.19 (b)CBR1(CGNSS) Time series

mode to determine the precise position and velocity of the continuous station. Time series of earlier CGPS station (CBRI) and the present CGNSS station (CBR1) is given in figure 6.19.

Shrungeshwar T S, Chiranjeevi Vivek G, Dharma Teja A K, Sunil Babu M G, Sridevi Jade and CBRI Team

6.14 Seismic hazard and risk assessment based on the Unified Scaling Law for earthquakes: State of Gujarat, India

The Gujarat region is located within the tectonic plate of India; about 500 km from a transform plate boundary (Bendick et al., 2001) is seismically one of the most active regions in India. The reliable assessment of seismic hazard of Gujarat is a major issue, particularly after the catastrophic Bhuj earthquake happened on January 26, 2001 (Mw7.7) resulting in a huge loss of lives (above 20,000 fatalities). There are many studies on seismic hazard assessment of Gujarat region in the recent past; however, none of these studies have been used to implement the associated seismic risk for the region. In this study, we not only combined and compared the seismic hazard from various probabilistic and neo-deterministic models but also integrated it with the population density data available after the 2011 census to assess the seismic risk of Gujarat region.

We apply the Unified Scaling Law for Earthquakes, USLE that generalizes the Gutenberg-Richter recurrence relation, has evident implications since any estimate of seismic hazard depends on the size of territory that is used for investigation, averaging, and extrapolation into the future. Therefore, the hazard may differ dramatically when scaled down to the proportion of the area of interest (e.g. a city) from the enveloping area of investigation.

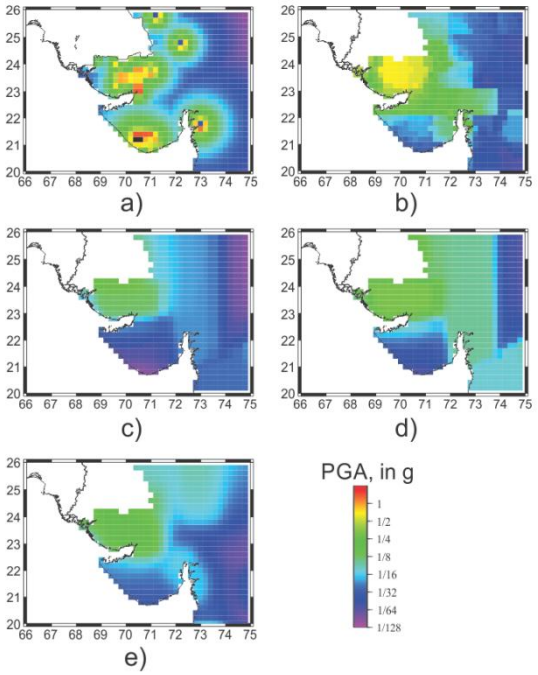

Figure 6.20 The five seismic hazard maps in terms of PGA (in g) a) based on USLE approach, b) DGA, c) DGA10%, d) DGA2%, e) as given on the final GSHAP seismic hazard map.

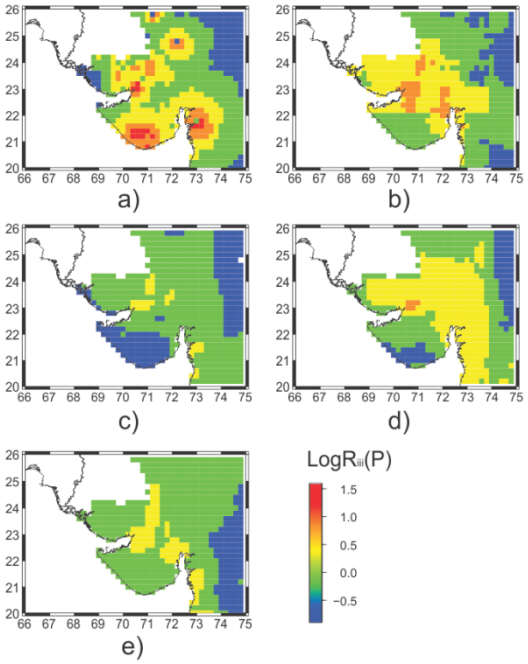

Figure 6.21 The maps of seismic risk $R_{iii}(g)$ for population of Gujarat region. Oversimplified convolutions, $R_{iii}(g) = H(g) \bullet \int_g P \bullet P^2$, of the India's Census 2011 population data with seismic hazard assessment H(g) based on USLE (a), b) DGA, c) DGA10%, d) DGA2%, e) GSHAP approaches (seismic hazard maps in Fig.6.20).

To assess a more adequate earthquake hazard for the state of Gujarat, we apply USLE and cross compare the seismic hazard maps compiled for the same standard regular grid 0.2°×0.2° (i) in terms of design ground acceleration (DGA) based on the neo-deterministic approach, (ii) in terms of probabilistic exceedence of peak ground acceleration (PGA) by GSHAP, and (iii) the one resulted from the USLE application (Figure 6.20). Finally, we present the maps of seismic risks for the state of Gujarat integrating the obtained seismic hazard, population density based on India's Census 2011 data, and a few model assumptions of vulnerability (Figure 6.21).

The present study for the State of Gujarat, India discloses a possibility of much higher risks than those on the existing probabilistic seismic hazard maps when naturally fractal distribution of earthquake loci is taken into account along with tectonic evidence and pattern recognition arguments. First of all it refers to the two areas to the North of continuation to the Arabian Sea of the Narmada-Son Lineament that crosses the entire Indian subcontinent; in particular, these are the areas to the North of Gimar Hills and Baroda Plane, where the USLE approach suggests

a possibility of significant or even great earthquakes. Further investigation of the Kathiawar Peninsula tectonic structure and dynamics along with pale-seismological searches may help with reliable information for resolving the problem of seismic safety in the region.

Imtiyaz A Parvez, Anastasia Nekrasova* and Vladimir Kossobokov*

**Institute of Earthquake Prediction Theory & Mathematical Geophysics, RAS, Moscow, Russian Federation*.

6.15 Crustal structure and seismicity beneath Kashmir Himalaya

Crustal structure and seismicity beneath the Kashmir valley are studied using data from eight broadband seismometers installed during 2013-2015. Moho depth and other intracrustal velocity contrasts are mapped from teleseismic data recorded at these stations. Local earthquakes are also analyzed both from first five month collected data and phase data obtained from International Seismological Centre (ISC) to understand the undergoing thrusting process in the region. A low velocity zone (LVZ) lies at the depth of ≈12-14 km beneath valley but upwarps slightly as we move further NE, which might be due to upthrusting of Zanskar shear zone and Dharlang shear zone. Moho beneath valley is (≈53-56 km) but steeply deepens beneath Pir Panjal and also towards NE.

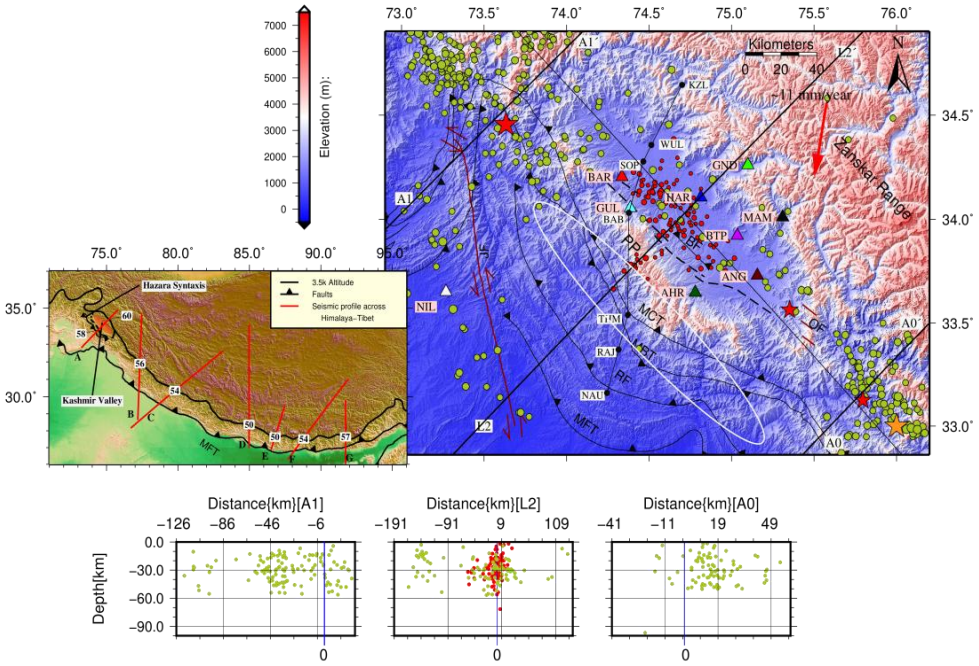

Figure 6.22 Main map shows Kashmir valley with stations by black triangles, brown color shows the relocated epicenters for M>=2.9 events whose phase data were obtained from ISC and red ones are the locally recorded events by our network which also have been relocated. White ellipse shows a possible rupture area of 1555 earthquake. Elevation data are taken from SRTM with scale shown on left. Red vector shows convergence rate of the Valley treated India fixed; stars are some recent earthquakes in the region. Black dots connected with lines are the record points of deep seismic sounding profile. NIL, is IRIS station in Nilore, Pakistan. Left inset shows map of the Himalayas with major faults with red rectangle highlighting the study region. Bottom shows the seismicity along different profiles with distances reckoned from axis of the valley (blue line). Note sparse seismicity towards NE of the valley which may be due to locking line beneath the Zanskar.

All the seismic stations (Figure 6.22) are located on hard rock sites of valley, three on its south-western and four adjoining its north-eastern margin. Receiver Functions (RFs) at these sites were calculated using iterative time domain deconvolution method and jointly inverted with surface wave dispersion data to estimate shear wave velocity structure underneath. The estimated Moho depths were further constrained within ±2 km by trial forward modeling. The Moho depths on the south- western edge of valley are close to 55 km (Figure 6.23), slightly shallower than the Pir Panjal further southwestward but about 15 km deeper than beneath sub-Himalaya about 30 km to southwest. The Moho depth increases to about 60 km towards its northeastern edge, indicating that here, as in the Central and Nepal Himalaya, the Indian plate dips north-eastwards beneath the Himalaya. A persistent low velocity interface at 12-16 km depth possibly delineates northward dipping decollement along which Tibet overrides the Indian plate. A total of 215 local earthquakes were located, which were further improved using Double-Difference algorithm. Earthquakes M≥2.9 with phase data for P and S arrivals were obtained from ISC (1964-2013).

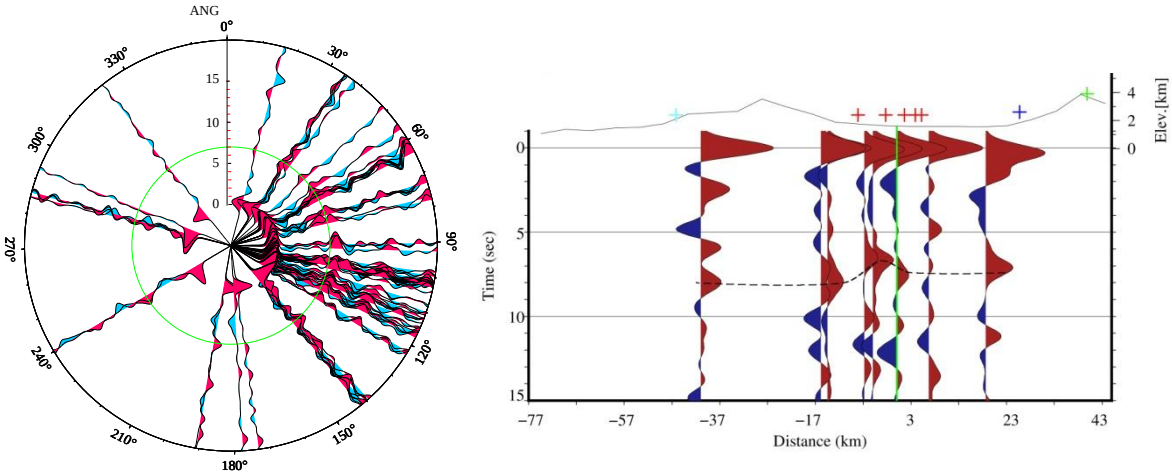

Figure 6.23 Left shows polar plot of RFs at station ANG, with vertical axis marking time in seconds. Note a positive phase arriving ~7sec, observable on most of RFs which marks the arrival of Moho Ps phase. Also note large gaps in back-azimuth (BAZ) between 140-170, 190-240, 240-280, 300-320, 330-360 degrees, which are due to absence of teleseismic events in those BAZ. Right shows selected RFs along SW-NE (from left-right) profile across the Kashmir Valley, with green line denoting axis of the Valley and distances along x-axis are measured w.r.t. the axis. Plus signs at top shows location of piercing points of different events recorded at different stations. Elevation data is taken from SRTM, note a spline fiited to Ps Moho phase showing upwarp of Moho beneath the Valley, Moho beneath Pir Panjal is slightly deeper than the Valley.

The Moho marking base of the valley apparently dips rather steeply ≈ 20°northeastwards of Main Boundary Thrust only to become very gentle ≈ 3.5° underneath valley but transition that must occur somewhere beneath Pir Panjal cannot be resolved by our data. Intriguingly, the Moho whilst generally dipping northeastward beneath valley shows a slight upwarp along its axis. A prominent low velocity interface at ≈ 12-16 km is also found to occur in most inversions of receiver functions and their existence is ineluctably required by forward modeling. It possibly identifies a piece of decollement beneath valley and holds promise to show existence of asperities on either side of valley on detailed exploration. The well constrained findings of this experiment are shear velocity structure beneath the valley obtained by jointly inverting RFs with

SWD data, further rigorously tested by forward modeling and set of relocated earthquakes which conform locking line beneath Valley.

Ramees R Mir, Imtiyaz A Parvez, Vinod K Gaur, Ashish, Rakesh Chandra* and Shakil A Romshoo*
**Department of Earth Sciences, University of Kashmir, Srinagar*

6.16 Moho imaging in Dharwar craton

The Indian shield is an amalgamation of smaller craton formed by geodynamic process from Mesoarchean to Neoproterozoic. Southern part of the shield is largely occupied by Dharwar craton (Figure 6.24). On the surface, craton is divided into the Western Dharwar Craton (WDC) and Eastern Dharwar Craton (EDC) separated by 2.5 Ga Closepet granite or Chitradurga Schist Belt (CSB) as boundary. In western Dharwar, CSIR-4PI had operated twelve broadband stations during 2010 and 2013 across the east – west corridor in two phases to image moho and Crustal structures along profile AA' (Figure 6.24). Data from Ten additional broadband stations, operated by CSIR – NGRI close to the profile AA', are also used in this study.

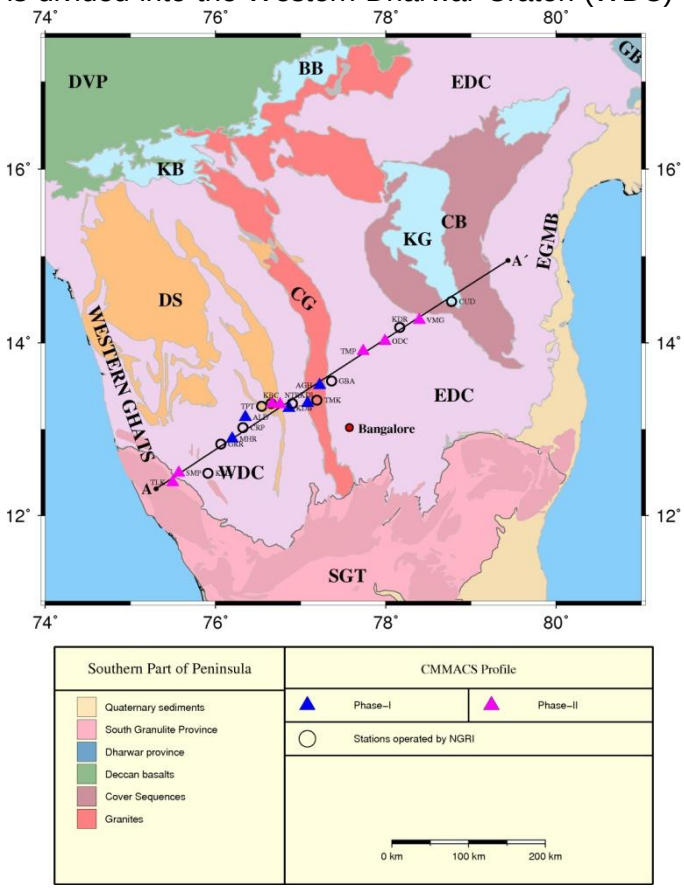

Figure 6.24 Geological map of the region showing major geological and tectonic features of Dharwar craton and location of broadband stations (pink, blue and black) used in this study. Profile AA' repersent the section along which station are projected. EDC: East Dharwar Craton; WDC: West Dharwar Craton; SGT: Southern Granulite Terrain; DS: Dharwar Schist; CG: Closepet granite; CB; Cuddapah Basin; KB: Kaladgi Basin; DVP: Deccan Volcanic Province; BB: Bhima Basin.

Broadband Stations data were recorded in continuous mode at 100 sps. Earthquake waveform were extracted for the teleseismic events occurred between 30^o to 100^o epicentral distance from the network. A total 22 stations were used in this study including stations from CSIR – NGRI. Receiver functions are generated for all the teleseismic waveform data for M > 5.5 and visually selected for final analysis. To estimate moho depth, three methodologies are used; H-K stacking, joint inversion of receiver function and Rayleigh wave group velocity data and CCP depth migration. H-K stacking used a grid search method, by adding amplitudes of Ps phase and its multiples, to estimate moho depth (H) and V_p/V_s ratio assuming average V_p of the crust. Joint inversion of

receiver functions were performed with Rayleigh wave group velocity to constrain moho depth and average velocity respectively. Receiver functions from 22 stations have been used to image the crust and upper mantle using Common Conversion Point (CCP) stacking technique to create time to depth migration of radial receiver functions.

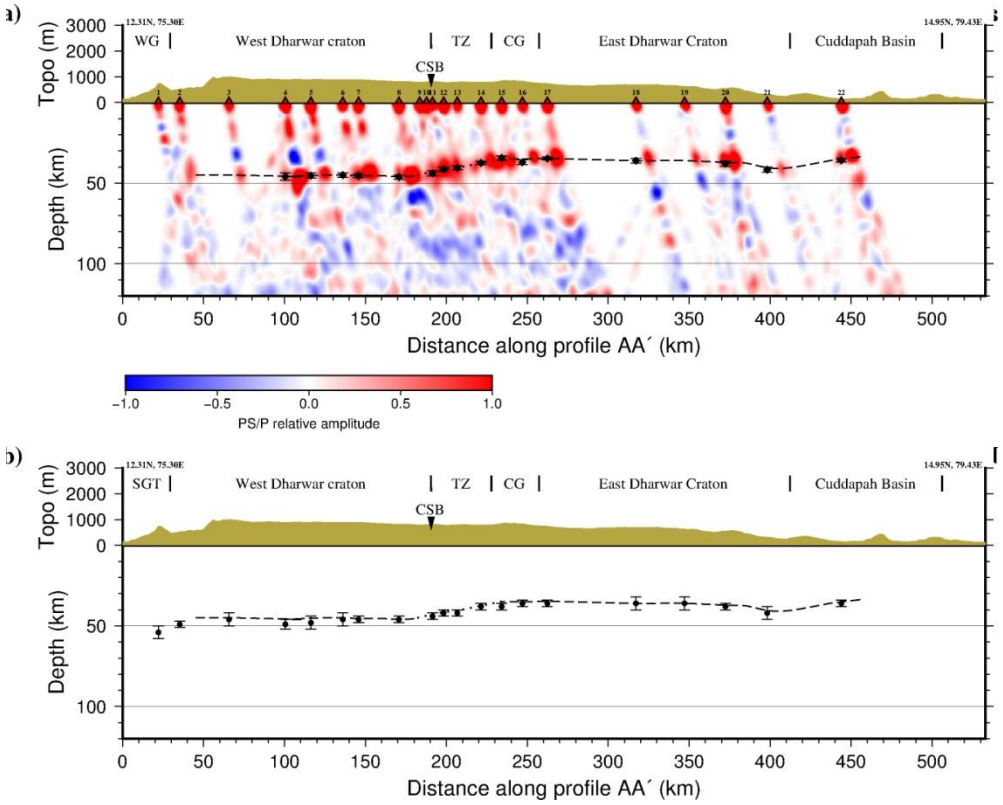

Figure 6.25 Common Conversion Point (CCP) Depth migration of receiver function along-with topography and tectonic feature projected along the profile AA'. (a) CCP depth Image along profile AA' along-with moho depth estimated from H-K stacking of receiver function. Interpreted moho marked by dashed black line. (b) showing moho depth along the profile estimated from joint inversion of receiver function and Rayleigh wave group velocity along with interpreted moho from CCP depth image.

The resulting CCP depth migration for profile AA' is plotted in Figure 6.25. The crust-mantle boundary is clearly visible beneath the Dharwar craton as the only laterally continuous strong amplitude positive interface (red). In east Dharwar, The general trend is flat Moho at a depth of 36--38 km. On the other hand in west Dharwar, Moho depth varies from 46--50 km and a presence of strong intra-crustal amplitude at a depth of ~15 km. Average Moho depth results are largely consistent with earlier studies carried out in the vicinity of profile. The Moho depth increase gradually between Colosepet granite and Chitradurga Schist Belt from station NTR and BRS. This section of profile is identified as a transition Zone (TZ) between EDC and WDC. The results also suggest moho offset at two places of an order of ~4--6 km; beneath EDC and west of Cuddapah Basin at station VMG; Beneath Western Ghat at station TLK. Results from H-K stacking and joint inversion are mostly consistent with CCP migrated results. Approx. 40 km

transition zone identified between CG and CSB, characterized by gradually increasing moho depth. This zone represents the contact between EDC and WDC between Chitradurga schist belt and Closepet granite and presence of intra-crustal structure coincide with Chitradurga schist belt.

Ashish and Imtiyaz A Parvez

6.17 Strong ground motion estimation in Western Himalaya & adjacent areas

Ground motion estimation can be done by various ways like deterministic, stochastic and hybrid methods. It is well known that slip on a fault is random in nature and high frequency waves appearing on a seismogram are difficult to generate using deterministic methods as they depend on small scale heterogeneities of the fault plane which further demands to incorporate more parameters thus augmenting the difficulty of using deterministic methods *(Aki, 1987)*. Also regions where no/less strong motion records are available use of stochastic methods seems to be a viable choice. An extended ruptures subfault motions can be computed efficiently using this method. Here gross features of the earthquake are quantified deterministically and details of the process are defined stochastically, particularly peak ground motions (peak acceleration etc.)

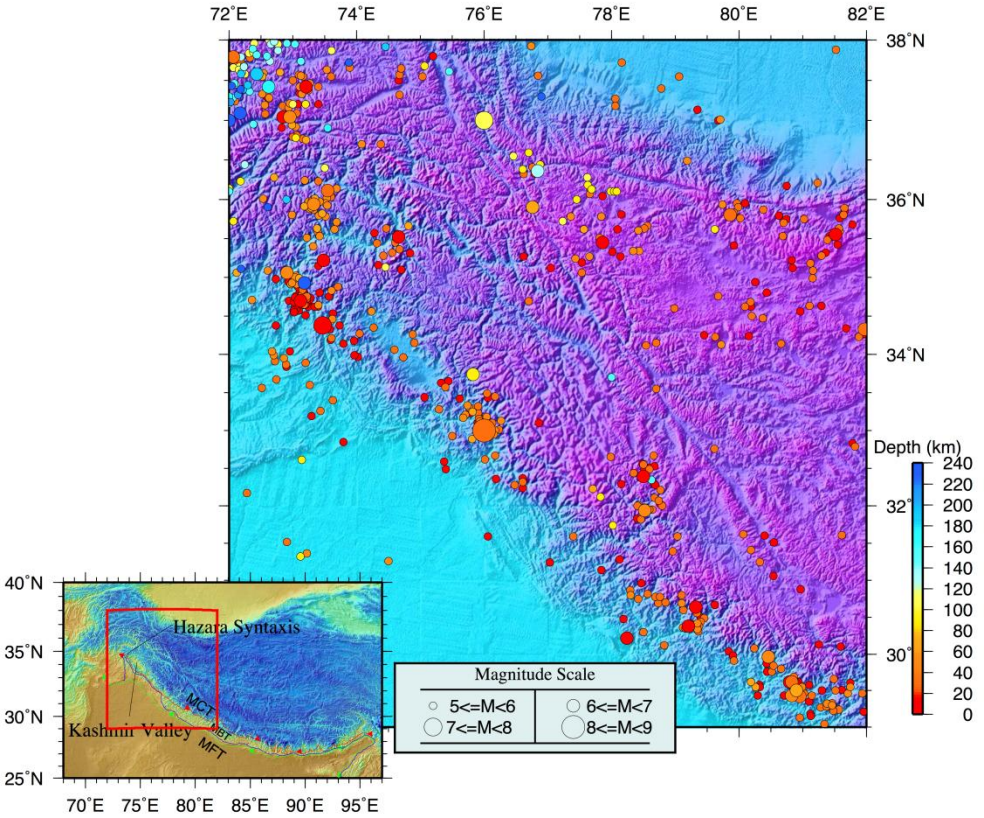

Figure 2.26 Shows seismicity map of NW Himalaya and adjacent areas for M≥5, pre-instrumental earthquakes have been taken from different sources. Each earthquake is color coded according to depth, notice deep events in Hindukush region. Inset shows the location of study region.

Ground motion has been generated using a finite fault stochastic modeling method. Here a finite fault is considered and is divided into number of subfaults, where each subfault is treated as a point source. Using random-vibration theory, peak values of ground motion are estimated and a random slip is chosen on all subfaults. Traditional stochastic estimation methods use a fixed corner frequency (f_{max}) of acceleration spectra. A dynamic corner frequency approach has been applied where rupture begins with a higher f_{max} and progresses towards lower f_{max}. It also uses an analytical method to simulate accurately near-fault ground motions by generating long-period pulses caused by the forward directivity of the rupture.

Above method will be used to generatesuites of ground motion in western Himalaya and adjacent areas by considering all M≥5 earthquakes in the region shown in Figure 2.26. For earthquakes M≤ 7, hypocentral depth is taken as 10 km, for 7<M<8 as 15 km and M≥ 8 as 25 km. We know that Kashmir Valley is covered by ~1300 m of sediments, site amplification will be considered and ground motion thus simulated will be compared with, when only considering rock and crustal amplification. Since we don't have any strong motion records of local/regional earthquakes from the region, we are using attenuation (Hypocentral distance vs acceleration) relations estimated for western Himalaya to validate our model. As this region has enough slip deficiency to drive a ~M8 earthquake and majority of the population within the Valley are located on loose sediments of the basin, this study will be important for the assessment of seismic hazard in the region. Figure 6.27 shows that after tuning of parameters in stochastic model, simulated ground motion is quite similar to the ground motion attenuation law of Western Himalayas.

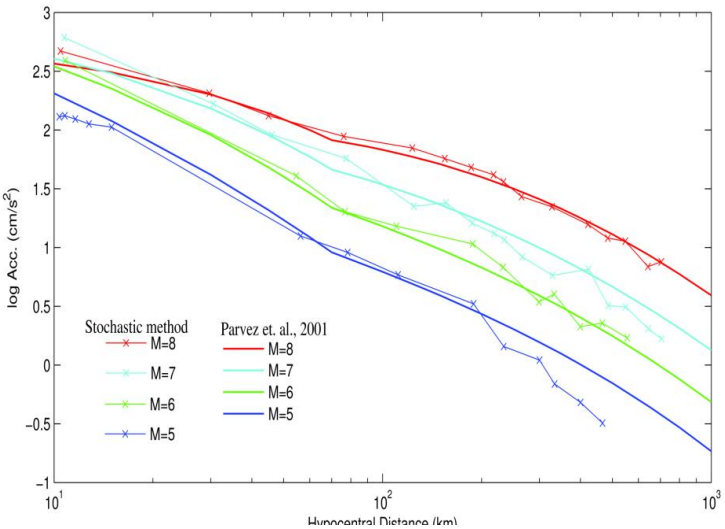

Figure 6.27 Shows the comparison of log acceleration (cm/s²) Vs Hypocentral distance (km) for Western Himalaya (solid lines, see legend) and stochastic method (line segments with crosses).

Ramees R Mir, Imtiyaz A Parvez, Vinod K Gaur

6.18 Study of tank with inclined braced staging

The responses of an intze tank with unbraced staging, inclined bracing (single-inclined brace and cross brace) at alternate levels of staging and inclined bracing throughout the height of staging have been compared. The models have been analyzed in accordance with the draft of IS 1893 (part 2) using STAAD. Pro a finite element software. The displacement of the tank reduced significantly when the staging had inclined braces. The study also found that the position of the inclined bracing in the staging (with and without bracing at ground level) had a considerable effect on the response of the tank. Liquid storage tanks are important structures

and it is imperative that these structures remain functional following an earthquake. Hence it is necessary to understand the behavior of the tanks under seismic loading. In this study, single-inclined braces and cross braces had been incorporated to the staging of the tank at alternate levels and their response had been compared with that of a tank with unbraced staging and single-inclined brace and cross brace throughout the height of staging.

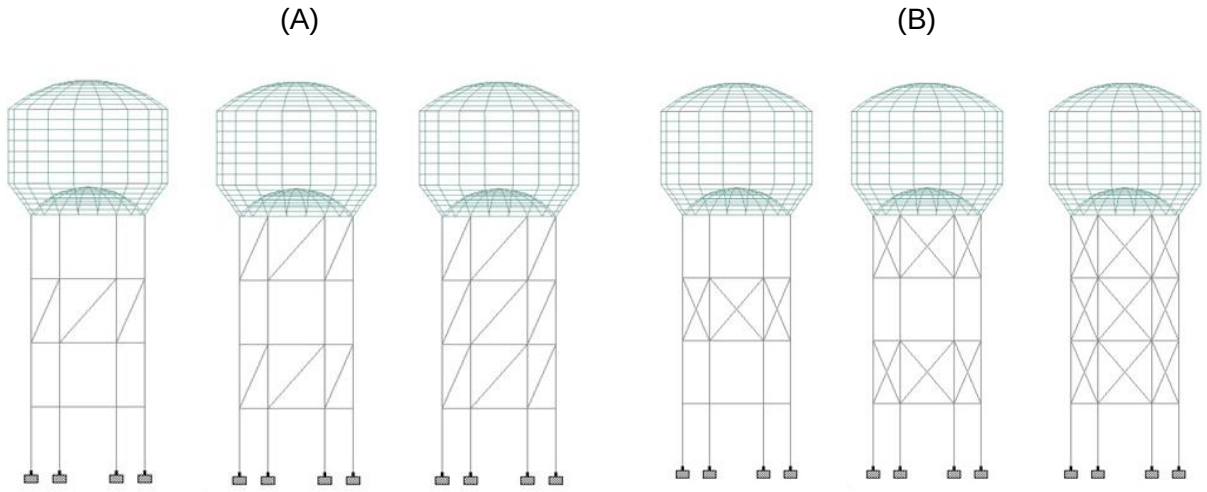

Figure 6.28 Intze Tank with type1, type2 and type3 for Single Braced (A) staging and Cross Based (B) of 16 m height

The liquid in the tank is divided into two liquids; one which moves with the wall of the tank container called impulsive liquid with mass m_i and the other that moves relative to the wall of the container called the convective liquid with mass m_c. The pressure exerted on the wall and base of the container by these liquids is called as hydrodynamic pressure. The elevated tank is treated as a two degree of freedom system, where one mass constitutes the impulsive mass along with the structural mass of the tank and the other constitutes the convective mass. The spring mass parameters depend on the aspect ratio of the tank and have been calculated using the draft of IS 1893 (part 2) and the IIT-GSDMA guidelines; analyzed for seismic zone II. A response reduction factor of 2.5 had been adopted as the frame was assumed to be a special moment resisting frame (SMRF) and an importance factor of 1.5 had been considered as per IS 1893 (Part 1). Figure 6.28 shows the configurations with inclined and crossed bracing at alternate levels of staging as type1 and type2 and the configuration with bracing throughout the height of staging is type3. Type1 configuration does not have bracing in the ground level whereas type2 has bracing at the ground level. On an average, the displacement of type1, type2 and type3 of single-diagonal braced and cross braced staging configurations was considerably less than the radial braced and horizontal cross braced staging configurations when the tanks were analyzed for self-weight of the structure, hydrostatic and hydrodynamic pressures in the container. Hence to reduce the displacement of an elevated tank, staging with cross bracing and single-diagonal bracing can be adopted instead of radial and horizontal-cross

bracing. The present study can be concluded that staging with single-diagonal bracing at alternate levels with bracing at ground level is a better alternative than the other staging configurations considered in this study.

6.19 Adaptive nonlinear pushover analysis on L-shaped building

The demand of reliable nonlinear static pushover analysis on structures subjected to earthquake forces has resulted in adaptive pushover analysis in the recent times, which considers the effect of higher modes of vibration and progressive stiffness degradation of structural members. The irregularities in the buildings are considered to be damage amplifiers since they make the failure in structures brittle during the incidence of an earthquake force. In Nonlinear static method, a mathematical model is simulated by incorporating the nonlinear characteristics like load-deformation relations into the constituent elements of the structure. The model is loaded with gravity loads and subjected to monotonically increasing lateral load representing the inertia forces in an earthquake. The structure will be pushed till the target displacement is exceeded at the control node. This conventional pushover method recommended by ATC-40 and FEMA-356 considers the only effect of the dominant mode of vibration. In the case of irregular structures, mainly in plan irregular buildings, the torsional mode of vibration will cause considerable damage to the structures during earthquake incidences. However, the effect of torsional mode of vibration will be neglected in conventional pushover analyses.

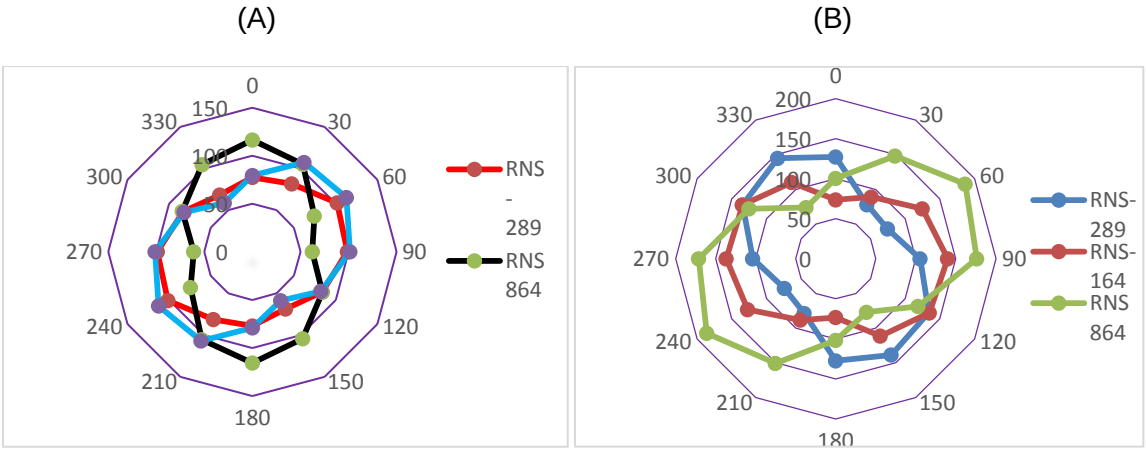

Figure 6.29 Maximum top displacements along X direction (A) and Y direction (B) for one of the Models for all bidirectional orthogonal earthquake components.

The consideration of higher mode of vibration led to the development of adaptive nonlinear static pushover analysis. Incorporation of adaptive methodology in the conventional pushover analysis is done in following steps. (1) Definition of nominal load vector and inertia force. (2) Calculation of load vector after the lateral load increment. (3) Calculation of scaling vector and updating the loading vector. The first step is carried out only at the beginning of the analysis and other steps are repeated at every equilibrium stage of the analysis is reached. Following the above-mentioned steps, the effect of higher modes of vibration is also taken into account in the

analysis. Figure 6.29 shows the variation of top displacement at the control node for the different angle of incidences. It is seen that for different earthquakes of same peak ground acceleration give the different angle of incidence of maximum response.

This study evaluates the performance of the plan irregular building (L-shaped) using nonlinear adaptive pushover when subjected to seismic forces. From the time history analysis along different direction shows that there is a significant variation in the response of the models considered with different angle of incidence. The critical angle of incidence depends on the chosen engineering parameter and the seismic input properties. This shows that there is a clear uncertainty in the definition of the critical angle.The uncertainty can be represented in the form of coefficient of variation, which is the ratio of standard deviation to mean demand value. This value varies from 0.16 to 0.36 confirming that variation in the seismic demand due to angle of incidence cannot be neglected.

Prajwal T P, Imtiyaz A Parvez and Kiran Kamath